Biocatalytic C=C Bond Reduction through Carbon Nanodot-Sensitized Regeneration of NADH Analogues

Kim, Jinhyun; Lee, Sahng Ha; Tieves, Florian; Choi, Da Som; Hollmann, Frank; Paul, Caroline E.; Park, Chan Beum

DOI
10.1002/anie.201804409

Publication date
2018

Document Version
Final published version

Published in
Angewandte Chemie - International Edition

Photobiocatalysis

International Edition: DOI: 10.1002/anie.201804409
German Edition: DOI: 10.1002/ange.201804409

Biocatalytic C=C Bond Reduction through Carbon Nanodot-Sensitized Regeneration of NADH Analogues

Jinhyun Kim, Sahng Ha Lee, Florian Tieves, Da Som Choi, Frank Hollmann, Caroline E. Paul, and Chan Beum Park**

Abstract: *Light-driven activation of redox enzymes is an emerging route for sustainable chemical synthesis. Among redox enzymes, the family of Old Yellow Enzyme (OYE) dependent on the nicotinamide adenine dinucleotide cofactor (NADH) catalyzes the stereoselective reduction of α,β-unsaturated hydrocarbons. Here, we report OYE-catalyzed asymmetric hydrogenation through light-driven regeneration of NADH and its analogues (mNADHs) by N-doped carbon nanodots (N-CDs), a zero-dimensional photocatalyst. Our spectroscopic and photoelectrochemical analyses verified the transfer of photo-induced electrons from N-CDs to an organometallic electron mediator (**M**) for highly regioselective regeneration of cofactors. Light triggered the reduction of NAD^+ and $mNAD^+$s with the cooperation of N-CDs and **M**, and the reduction behaviors of cofactors were dependent on their own reduction peak potentials. The regenerated cofactors subsequently delivered hydrides to OYE for stereoselective conversions of a broad range of substrates with excellent biocatalytic efficiencies.*

Ene reductases from the Old Yellow Enzyme (OYE) family catalyze the asymmetric reduction of activated C=C bonds in α,β-unsaturated compounds.[1] The oxidoreductase contains a flavin mononucleotide (FMN) prosthetic group to which a hydride is transferred from a reduced nicotinamide adenine dinucleotide cofactor [NAD(P)H]. Subsequently, the substrate is *trans*-hydrogenated by accepting a hydride from the reduced FMN and a proton from a Tyr-residue of the OYE. Despite the potential of OYE-catalyzed asymmetric reduction, the provision of stoichiometric NAD(P)H makes the process economically not feasible due to the high price of the cofactor.[2] This issue has prompted studies on in situ conversion of $NAD(P)^+$ to its reduced form (or vice versa) using different methods (e.g., enzymatic, chemical, electrochemical, photochemical, and photoelectrochemical).[3] According to the literature,[4] the use of hydride-transfer mediators can facilitate regioselective regeneration of NAD(P)H by avoiding the formation of enzymatically inactive NAD dimers. Furthermore, the mediators can function as a diffusing communicator between photoactive materials and redox enzymes. As a substitute of the natural cofactor, synthetic nicotinamide cofactor analogues (mNADHs) have sparked a renewed interest in the field of redox biocatalysis because of their low price, better chemical stability, and even improved biocatalytic efficiency.[5] Several studies have demonstrated applications of the analogues as electron donors to drive various redox enzymes (e.g., monooxygenase, P450 BM-3, enoate reductase, malate dehydrogenase, D-lactate dehydrogenase, and malic enzyme).[5]

Here, we report photoactivation of OYEs through light-driven regeneration of mNADHs using carbon nanodots (CDs) as a photosensitizer, as depicted in Scheme 1. Three different $mNAD^+$s have been synthesized for this study: 1-benzyl-3-carbamoylpyridinium (mNH_2^+), 1-butyl-3-carbamoylpyridinium (mBu^+), and 1-benzyl-3-carboxypyridinium ion ($mCOOH^+$). According to the literature,[5,6] these analogues possess one or two substituted functional groups positioned on C3 and/or N1 atoms that give rise to different kinetic parameters for the reductive reactions catalyzed by OYEs. We employed triethanolamine (TEOA) and Cp*Rh(bpy)H_2O^{2+} (Cp* = C_5Me_5, bpy = 2,2′-bipyridine) (**M**) as an electron donor and an electron mediator, respectively, for regioselective regeneration of mNADHs. Semiconducting materials such as quantum dots have been used for enzyme-mediated sensing, photobiocatalysis, and bioenergetic applications.[7] Nano-sized CDs are zero-dimensional carbonaceous semiconducting nanomaterials that exhibit UV/Vis absorptivity, good photostability, biocompatibility, water solubility, and tunable fluorescence emissions,[8] making them a prospective alternative to molecular dyes and semiconductor quantum dots for photocatalytic applications, such as CO_2 reduction,[9] H_2 evolution,[10] and water splitting.[11] Recently, CDs have been applied to photoenzymatic synthesis through their coupling with redox enzymes. For example, positively charged CDs were hybridized electrostatically with fumarate reductase for light-driven hydrogenation of fumarate to succinate via direct transfer of photoexcited electrons.[12]

We synthesized nitrogen-doped CDs (N-CDs) by one-pot hydrothermal treatment (200 °C, 5 h) of citric acid and ethylenediamine as a carbonaceous precursor and a nitrogen doping agent, respectively,[13] and characterized them using multiple analytical tools (see Figures S1–S6 in the Supporting

[*] J. Kim, Dr. S. H. Lee, D. S. Choi, Prof. Dr. C. B. Park
Department of Materials Science and Engineering, Korea Advanced Institute of Science and Technology (KAIST)
335 Science Road, Daejeon 305–701 (Republic of Korea)
E-mail: parkcb@kaist.ac.kr
Dr. C. E. Paul
Laboratory of Organic Chemistry, Wageningen University & Research
Stippeneng 4, 6708 WE Wageningen (The Netherlands)
E-mail: caroline.paul@wur.nl
Dr. F. Tieves, Prof. Dr. F. Hollmann
Department of Biotechnology, Delft University of Technology
Van der Maasweg 9, 2629 HZ Delft (The Netherlands)
Supporting information and the ORCID identification number(s) for the author(s) of this article can be found under https://doi.org/10.1002/anie.201804409.

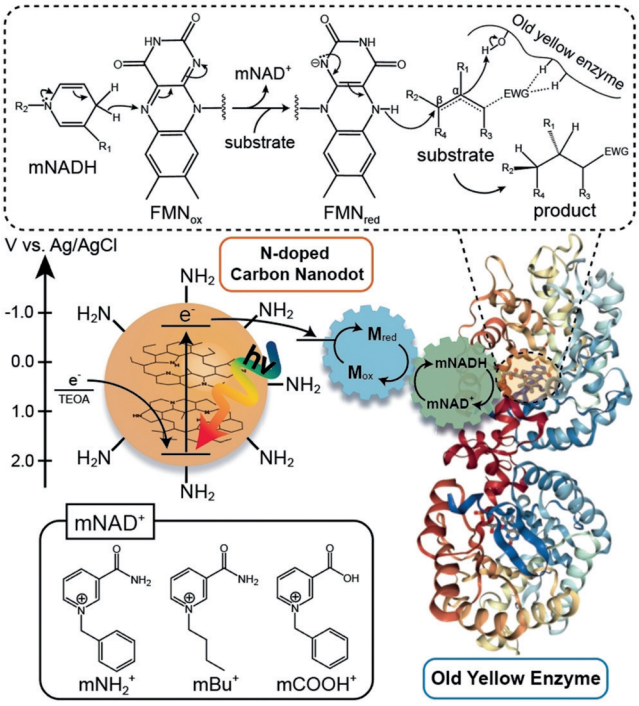

Scheme 1. Illustration of the photoenergy conversion into chemical energy by integrating photocatalysis and biocatalysis. Photoexcited electrons generated by N-doped carbon nanodots reduce the oxidized rhodium-based complex ($\mathbf{M}_{ox}$) that regioselectively converts $mNAD^+$ into mNADH. Subsequently, the enzymatically active mNADH returns to its oxidized form after donating a hydride to a prosthetic group (i.e., flavin mononucleotide, FMN) in the old yellow enzyme. The reduced FMN transfers a hydride onto Cβ of a substrate while a Tyr-residue gives a proton onto Cα, resulting in the *trans*-specific reduction of an activated C=C bond. EWG: electron-withdrawing group.

Information). According to the UV/Vis spectrum in Figure S7a, N-CDs exhibited UV absorption with tailing toward the visible light region. The corresponding Tauc plot in Figure S7b indicates that the optical band gap of N-CDs is approximately 2.74 eV. Figure S8 shows the onset of reduction potential, from which the corresponding LUMO was calculated to be −0.83 V (vs. Ag/AgCl). A HOMO of 1.91 V (vs. Ag/AgCl) was estimated based on the optical band gap value. This electronic configuration suggests photoactivated N-CDs possess the thermodynamic driving force to reduce **M** (redox potential of **M**: −0.76 V vs. Ag/AgCl[14]). To verify the transfer of photoexcited electrons from N-CDs to **M**, we obtained PL spectra of N-CDs with **M** in varying concentrations. According to Figure S9a, oxidative fluorescence quenching of N-CDs by **M** was observed, and the corresponding Stern–Volmer plot (Figure S9b) displayed a quadratic function of **M**. It suggests that the quenching of N-CDs resulted from the transfer of photoexcited electrons to **M** and the formation of an electrostatic complex between a negatively charged N-CD and a positively charged **M**. Furthermore, we obtained transient photocurrent responses of N-CDs to procure additional evidence of N-CD-sensitized reduction of **M** (Figure S10), which shows that the photoexcited electrons of N-CDs are delivered to mNH_2^+ via **M** upon light irradiation.

We investigated light-driven regeneration of mNADHs by N-CDs under illumination ($\lambda_{cut\text{-}on}$: 324 nm) in the presence of **M** and TEOA. The reduction of $mNAD^+$s to mNADHs was detected with different yields (in the order of NADH > mNH_2H > mBuH > mCOOHH). Detailed regeneration performances (e.g., total turnover number (TTN), turnover frequency (TOF)) are listed in Table S1. TEOA was selected as a sacrificial electron donor because its oxidation potential (ca. 0.86 V vs. Ag/AgCl)[7b] is more negative than the HOMO of N-CDs, and its suitability was confirmed by the reductive fluorescence quenching of N-CDs (Figure S11). Control experiments in the absence of each component (i.e., N-CDs, light, **M**, cofactor, and TEOA) resulted in no formation of NADH or mNADHs (Figure S12). This result indicates that light promotes the electrons of N-CDs to higher energy states that reduce **M** for mNADH regeneration, while the holes created by excited electrons are filled at the expense of TEOA oxidation. We also examined the dependency of the initial rate of cofactor regeneration on the intensity of incident light (Figure S13) and the concentration of N-CDs, **M**, cofactor, and TEOA, respectively (Figure S14).

We explored the differential catalytic efficiency of **M** toward each cofactor using cyclic voltammetric analysis. The degree of **M** mediation in the reduction of a cofactor was estimated by measuring the increase in the reduction peak current of **M** ($I_{M,p}$). According to Figures 1a and S15, the

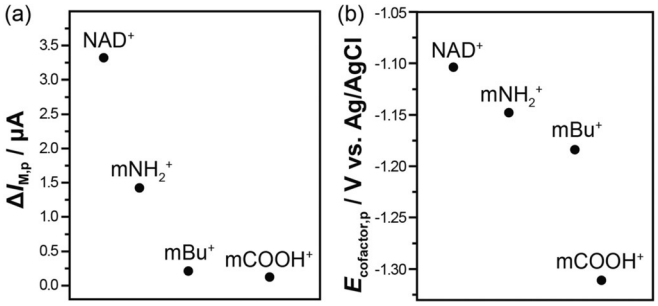

Figure 1. a) Comparison of changes in the cathodic peak current of 500 μM **M** ($\Delta I_{M,p}$) in the presence of 400 μM cofactor. b) Comparison of different reduction peak potentials of cofactors ($E_{cofactor,p}$). The electrochemical analysis was carried out in a phosphate buffer (100 mM, pH 7.5) at a scan rate of 50 $mV\,s^{-1}$. Working electrode: a polished glassy carbon electrode.

positive $\Delta I_{M,p}$ was in the order of $NAD^+ > mNH_2^+ > mBu^+ > mCOOH^+$. From a thermodynamic point of view, we ascribe the order to the different reduction peak potentials ($E_{cofactor,p}$) of oxidized cofactors in the order of $NAD^+ > mNH_2^+ > mBu^+ > mCOOH^+$ (Figures 1b and S16) because the driving force of **M** to reduce a cofactor becomes higher with a lower negative $E_{cofactor,p}$. On the molecular level, nicotinamide-based cofactors (i.e., NAD^+, mNH_2^+, mBu^+) contain the common amide functionality on C3 atom that is well known for the coordination to the Rh metal center of **M**. However, compared to NAD^+, different substituents of cofactor analogues on N1 atom exhibit lower electron-withdrawing abilities[15] in the order of ribosyl (of NAD^+) > 1-benzyl (of mNH_2^+) > 1-butyl (of mBu^+), making the pyridine ring less

electrophilic and less liable to accept electrons, resulting in higher negative $E_{cofactor,p}$ than that of NAD^+. On the other hand, $mCOOH^+$ possesses the negatively charged carboxyl group on C3 atom (at pH 7.5) that can interrupt the desirable carbonyl *O*-Rh coordination for hydride transfer due to the ionic interactions between the carboxyl group and the metal center of **M**.[16] We further investigated the effect of protonated carboxyl group of $mCOOH^+$ on the catalytic efficiency of **M** (Figure S17).

Next, we studied *trans*-hydrogenation of conjugated C=C bonds by implementing the photochemical recycling of cofactors into the biocatalysis driven by an OYE from *Thermus scotoductus* (*Ts*OYE). Figure S18 shows a progressive reduction of 2-methyl-2-cyclohexen-1-one with different production yields (in the order of mNH_2H > NADH > mBuH > mCOOHH) under illumination ($\lambda_{cut\text{-}on}$: 324 nm) for 180 min. As shown in Figure 2a, mNH_2H regeneration displayed the highest TOF_{TsOYE} of 511.8 h^{-1} and TTN_{TsOYE} of 670.1 among four different cofactors. The absence of cofactor (i.e., **M** alone) caused a failure in the *Ts*OYE-driven reduction of C=C bonds. The result indicates that NADH and mNADHs, not **M**, are the diffusing hydride donors to the prosthetic FMN in *Ts*OYE. We also observed that the photobiocatalytic performance increased with the concentration of N-CDs, indicating that a higher regeneration rate of mNH_2H enhances the rate and the production yield of OYE-driven *trans*-hydrogenation (Figure S19); TOF_{TsOYE} of 576.3 h^{-1} and TTN_{TsOYE} of 838.9 were achieved by using 0.20 mg mL^{-1} N-CDs. These values are much higher compared to other systems reported for photoactivation of OYEs (Table 1). We attribute the inverted order to the better kinetic parameters of mNADHs. According to the literature,[6] the catalytic efficiency for the reductive half-reaction (k_{red}/K_D) of *Ts*OYE with mNH_2H (533 $mM^{-1}s^{-1}$) is around three times higher than with NADH (163 $mM^{-1}s^{-1}$). In addition, the lower biocatalytic performance could be caused by chemical binding of NADH to N-CDs that possibly prohibits NADH from diffusing inside the catalytic site of *Ts*OYE (Figure S20). Furthermore, we examined the general applicability of the N-CD-sensitized photobiocatalytic platform to the conversion of another α,β-unsaturated compound (i.e., *trans*-cinnamaldehyde) by *Ts*OYE. In agreement with the conversion of 2-methyl-2-cyclohexen-1-one, the regeneration platform prompted *Ts*OYE activity toward the reduction of the unsaturated aldehyde with varying yields in the order of mNH_2H > NADH > mBuH > mCOOHH (Figure 2b). Compared to the reaction of 2-methyl-2-cyclohexen-1-one, the lower catalytic performance is ascribed to the inhibitory effect of the product 3-phenylpropionaldehyde on *Ts*OYE.[17] Taken together, N-CD-sensitized regeneration of NADH and its analogues can be applied to different unsaturated compounds and best results were obtained with mNH_2H compared to the natural cofactor and other analogues.

Table 1: Comparison of photobiocatalytic efficiencies for asymmetric reduction of activated C=C bonds in α,β-unsaturated compounds.

Photocatalytic system	OYE type	TOF_{OYE} [h^{-1}]	TTN_{OYE}	Yield [%]
N-CD-sensitized regeneration of mNH_2H (this study)[a]	*Ts*OYE	576.3	838.9	> 99
Eosin Y-sensitized direct activation of OYE[17]	*Ts*OYE	118.0	295.0	67
$[Ru(bpz)_2dClbpy]Cl_2$-sensitized regeneration of methyl viologen[18]	TOYE	121.5	500.0[b]	> 99
	PETNR	100.4	445.0[b]	89
CdSe-sensitized regeneration of methyl viologen[19]	YqjM	23.3[b]	8.0[b]	12[b]
Au-TiO_2-sensitized regeneration of free FMN[20]	*Ts*OYE	82.2[b]	411.2[b]	62[b]

[a] With 0.20 mg mL^{-1} N-CDs (Figure S19). [b] Approximate estimation based on data provided by the corresponding reference.

In summary, we have demonstrated OYE-catalyzed asymmetric hydrogenation by N-CDs via light-driven regeneration of NADH and its analogues (i.e., mNH_2H, mBuH, and mCOOHH). Through spectroscopic and (photo)electrochemical analyses, we elucidated the capability of N-CDs to deliver photoexcited electrons to **M** and different photochemical reduction behaviors of NAD^+ and $mNAD^+$s. Initial rates and yields of regeneration were in the order of NADH > mNH_2H > mBuH > mCOOHH, which we ascribe to different reduction peak potentials of cofactors. The coupling of photochemical regeneration of mNADHs with a *Ts*OYE-driven reaction allowed for the efficient synthesis of (*R*)-2-

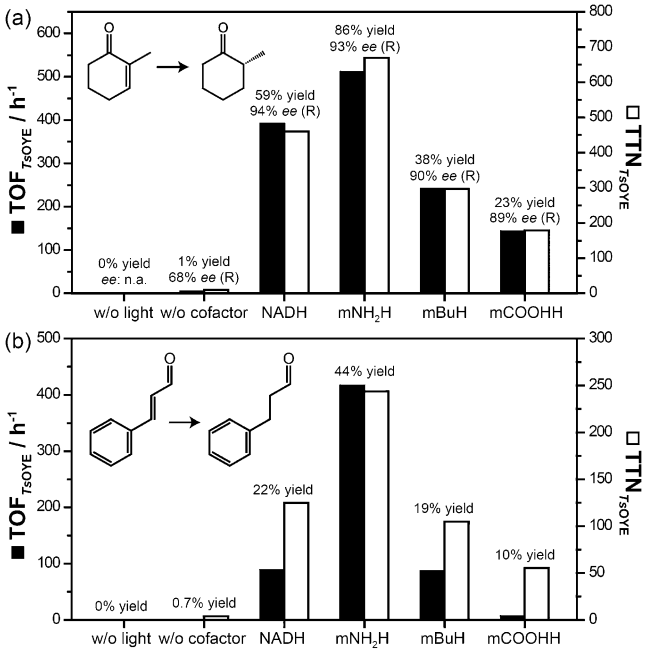

Figure 2. a) N-CD-sensitized photobioenzymatic reduction of (a) 2-methyl-2-cyclohexen-1-one (7 mM) and (b) *trans*-cinnamaldehyde (5 mM) by *Ts*OYE. Reaction conditions: N-CDs (0.10 mg mL^{-1}), **M** (25 μM), substrate, cofactor (2 mM), *Ts*OYE (9 μM), and $CaCl_2$ (5 mM) in a TEOA buffer (500 mM, pH 7.5) at 45 °C. Light intensity: 200 mW cm^{-2}. Light source: a xenon lamp equipped with a 324 nm cut-on optical filter. TOF was determined after (a) 30 min and (b) 15 min of reaction. TTN and *ee* were determined after (a) 180 min and (b) 75 min of reaction.

methylcyclohexanone (≈94% *ee*). Furthermore, a broader applicability of the photobiocatalytic system was demonstrated by employing different substrates (e.g., 2-methyl-2-cyclohexen-1-one, *trans*-cinnamaldehyde). The photochemical regeneration platform of mNH_2H enabled excellent catalytic activities of *Ts*OYE over the substrates. Compared to other cofactors, mNH_2H's excellent performance is on account of the higher k_{red}/K_D of *Ts*OYE with mNH_2H that compensates for the lower efficiency of mNH_2H regeneration. Although our photobiocatalytic system recorded a higher enzymatic efficiency than other platforms for light-induced activation of OYEs, admittedly it still falls short of the productivities obtained with classical cofactor regeneration systems.[21] Nevertheless, the limitations identified in this contribution are the basis for further improvements, such as the design of CDs exhibiting enhanced efficiencies of charge separation and migration, and the structural modification of the hydride-transfer mediator to tune its redox potential.[14] Overall, the light-driven approach to regenerate better-than-nature cofactor analogues is a promising strategy for efficient activation of oxidoreductases using light energy.

Acknowledgements

This work was supported by the National Research Foundation (NRF) via the Creative Research Initiative Center (Grant number: NRF-2015 R1A3A2066191), Republic of Korea, for C.B.P. and the Netherlands Organisation for Scientific Research by a VICI grant (Grant number: 724.014.003) for F.H. and a VENI grant (Grant number: 722.015.011) for C.E.P.

Conflict of interest

The authors declare no conflict of interest.

Keywords: alkene hydrogenation · asymmetric catalysis · carbon nanodot · NADH analogues · photobiocatalysis

How to cite: *Angew. Chem. Int. Ed.* **2018**, *57*, 13825–13828
Angew. Chem. **2018**, *130*, 14021–14024

[1] C. K. Winkler, G. Tasnádi, D. Clay, M. Hall, K. Faber, *J. Biotechnol.* **2012**, *162*, 381–389.
[2] a) J. H. Kim, D. H. Nam, C. B. Park, *Curr. Opin. Biotechnol.* **2014**, *28*, 1–9; b) S. H. Lee, J. H. Kim, C. B. Park, *Chem. Eur. J.* **2013**, *19*, 4392–4406.
[3] a) F. Hollmann, I. W. C. E. Arends, K. Buehler, *ChemCatChem* **2010**, *2*, 762–782; b) S. K. Kuk, R. K. Singh, D. H. Nam, R. Singh, J.-K. Lee, C. B. Park, *Angew. Chem. Int. Ed.* **2017**, *56*, 3827–3832; *Angew. Chem.* **2017**, *129*, 3885–3890; c) Y. Okamoto, V. Köhler, C. E. Paul, F. Hollmann, T. R. Ward, *ACS Catal.* **2016**, *6*, 3553–3557.
[4] "Electrochemistry of NAD(P)$^+$/NAD(P)H": L. Gorton, E. Domínguez, *Encyclopedia of Electrochemistry*, Wiley-VCH, Weinheim, **2007**, pp. 67–143.
[5] C. E. Paul, I. W. C. E. Arends, F. Hollmann, *ACS Catal.* **2014**, *4*, 788–797.
[6] T. Knaus, C. E. Paul, C. W. Levy, S. de Vries, F. G. Mutti, F. Hollmann, N. S. Scrutton, *J. Am. Chem. Soc.* **2016**, *138*, 1033–1039.
[7] a) M. Riedel, N. Sabir, F. W. Scheller, W. J. Parak, F. Lisdat, *Nanoscale* **2017**, *9*, 2814–2823; b) K. Schubert, W. Khalid, Z. Yue, W. J. Parak, F. Lisdat, *Langmuir* **2010**, *26*, 1395–1400; c) N. Sabir, N. Khan, J. Völkner, F. Widdascheck, P. del Pino, G. Witte, M. Riedel, F. Lisdat, M. Konrad, W. J. Parak, *Small* **2015**, *11*, 5844–5850; d) S. H. Lee, D. S. Choi, S. K. Kuk, C. B. Park, *Angew. Chem. Int. Ed.* **2018**, *57*, 7958–7985; *Angew. Chem.* **2018**, *130*, 8086–8116; e) R. Jungki, L. S. Ha, N. D. Heon, P. C. Beum, *Adv. Mater.* **2011**, *23*, 1883–1888; f) S. H. Lee, J. Ryu, D. H. Nam, C. B. Park, *Chem. Commun.* **2011**, *47*, 4643–4645; g) J. H. Kim, S. Y. Lim, D. H. Nam, J. Ryu, S. H. Ku, C. B. Park, *Biosens. Bioelectron.* **2011**, *26*, 1860–1865; h) D. H. Nam, S. H. Lee, C. B. Park, *Small* **2010**, *6*, 922–926; i) K. K. Sakimoto, A. B. Wong, P. Yang, *Science* **2016**, *351*, 74–77.
[8] G. A. M. Hutton, B. C. M. Martindale, E. Reisner, *Chem. Soc. Rev.* **2017**, *46*, 6111–6123.
[9] L. Cao, S. Sahu, P. Anilkumar, C. E. Bunker, J. Xu, K. A. S. Fernando, P. Wang, E. A. Guliants, K. N. Tackett, Y.-P. Sun, *J. Am. Chem. Soc.* **2011**, *133*, 4754–4757.
[10] a) B. C. M. Martindale, G. A. M. Hutton, C. A. Caputo, E. Reisner, *J. Am. Chem. Soc.* **2015**, *137*, 6018–6025; b) B. C. M. Martindale, E. Joliat, C. Bachmann, R. Alberto, E. Reisner, *Angew. Chem. Int. Ed.* **2016**, *55*, 9402–9406; *Angew. Chem.* **2016**, *128*, 9548–9552; c) B. C. M. Martindale, G. A. M. Hutton, C. A. Caputo, S. Prantl, R. Godin, J. R. Durrant, E. Reisner, *Angew. Chem. Int. Ed.* **2017**, *56*, 6459–6463; *Angew. Chem.* **2017**, *129*, 6559–6563.
[11] J. Liu, Y. Liu, N. Liu, Y. Han, X. Zhang, H. Huang, Y. Lifshitz, S.-T. Lee, J. Zhong, Z. Kang, *Science* **2015**, *347*, 970–974.
[12] G. A. M. Hutton, B. Reuillard, B. C. M. Martindale, C. A. Caputo, C. W. J. Lockwood, J. N. Butt, E. Reisner, *J. Am. Chem. Soc.* **2016**, *138*, 16722–16730.
[13] J. Bian, C. Huang, L. Wang, T. Hung, W. A. Daoud, R. Zhang, *ACS Appl. Mater. Interfaces* **2014**, *6*, 4883–4890.
[14] V. Ganesan, D. Sivanesan, S. Yoon, *Inorg. Chem.* **2017**, *56*, 1366–1374.
[15] H. C. Lo, O. Buriez, J. B. Kerr, R. H. Fish, *Angew. Chem. Int. Ed.* **1999**, *38*, 1429–1432; *Angew. Chem.* **1999**, *111*, 1524–1527.
[16] S. H. Lee, H. J. Lee, K. Won, C. B. Park, *Chem. Eur. J.* **2012**, *18*, 5490–5495.
[17] S. H. Lee, D. S. Choi, M. Pesic, Y. W. Lee, C. E. Paul, F. Hollmann, C. B. Park, *Angew. Chem. Int. Ed.* **2017**, *56*, 8681–8685; *Angew. Chem.* **2017**, *129*, 8807–8811.
[18] M. K. Peers, H. S. Toogood, D. J. Heyes, D. Mansell, B. J. Coe, N. S. Scrutton, *Catal. Sci. Technol.* **2016**, *6*, 169–177.
[19] T. N. Burai, A. J. Panay, H. Zhu, T. Lian, S. Lutz, *ACS Catal.* **2012**, *2*, 667–670.
[20] M. Mifsud, S. Gargiulo, S. Iborra, I. W. C. E. Arends, F. Hollmann, A. Corma, *Nat. Commun.* **2014**, *5*, 3145.
[21] H. S. Toogood, T. Knaus, N. S. Scrutton, *ChemCatChem* **2014**, *6*, 951–954.

Manuscript received: April 15, 2018
Revised manuscript received: June 20, 2018
Accepted manuscript online: July 30, 2018
Version of record online: August 29, 2018

